

The Impact of Dose Calculation Algorithm for SBRT Lung Cancer Radiotherapy Treatment

Ahmed Ali Mostafa^{1*}, Abd El-Azeem Elmorcy Hussein², Mohamed Mahmoud Galal³, Khaled Mohammed El-Shahat⁴

1. Kafr Ash shaykh military oncology center, Egypt
2. Menoufia University, faculty of science, department of Physics, Egypt
3. Hermitage Medical Clinic, Physics department, Dublin, Ireland
4. Al Azhar University, faculty of medicine, Oncology department, Egypt

ARTICLE INFO	ABSTRACT
<p>Article type: Original Paper</p> <hr/> <p>Article history: Received: Apr 03, 2021 Accepted: Sep 15, 2021</p> <hr/> <p>Keywords: Radiotherapy Planning Stereotactic Body Radiotherapy Lung Neoplasms Anisotropic analytical Algorithm Acuros XB Algorithm</p>	<p>Introduction: The study aimed to provide the dose accuracy effects between the Anisotropic Analytical Algorithm (AAA) and the deterministic solver Acuros XB (AXB) that are available on Eclipse TPS (Varian Medical Systems, Palo Alto, CA) treatment planning system (TPS). The purpose is to investigate the difference between the AAA and Acuros XB Algorithm, The difference is due to the electron transport difference in the case of small fields.</p> <p>Material and Methods: For the study of non-small cell lung cancer (NSCLC) patient Computed tomography (CT) scans are used to do retrospective stereotactic body radiosurgery (SBRT) plans via AAA and recalculated by AXB dose calculation algorithms using the Eclipse treatment planning system. The main dosimetric comparison parameters are Conformity index (CI), Homogeneity Index (HI), Gradient Index (GI), Target mean dose, and calculation time. The Statistical analysis done by the gamma index comparison.</p> <p>Results: Based on the results, the CI is (1.45±0.55) to (1.85±0.7) (P<0.05). The HI are (0.15±0.07) and (0.13±0.08) (P<0.05), the GI for AAA was (4.8±2.6) and for AXB reaches (7.4±3.8) (P<0.05) and the maximum dose for Planning target volume (PTV) is differed about 2.3% to 4.5%, mean dose is differed about 2.4% to 3.8% and the calculation time 153±43sec and 185±76sec for AAA and AXB respectively.</p> <p>Conclusion: The findings using the deterministic solver AXB in the calculation for the case of low density like lung cases is more accurate than AAA calculation Algorithm in SBRT treatment.</p>

► Please cite this article as:

Mostafa AA, Hussein AA, Galal MM, El-Shahat Kh. The Impact of Dose Calculation Algorithm for SBRT Lung Cancer Radiotherapy Treatment. Iran J Med Phys 2022; 19: 290-295. 10.22038/IJMP.2021.56733.1951.

Introduction

Stereotactic body radiotherapy (SBRT) is an effective way of treating individuals with early-stage non-small cell lung cancer (NSCLC) who are clinically inoperable or refuse surgery [1]. SBRT is usually performed in one to five sessions over one to two weeks [2, 3]. SBRT utilizes various beams to create a highly conformal dose distribution with rapid fall off at the target's periphery, resulting in less toxicity to healthy tissues around. As there is a clear association between tumor local control and SBRT dose delivered, [4-6], It is critical to apply an accurate and highly conformal dose to the target. SBRT needs a high level of accuracy for all stages of the treatment process [7], with an evaluation and assessment of the different algorithms used in dose calculation. So this research aims to investigate the different between the AAA and Acuros XB Algorithm.

AAA Dose Calculation Algorithm

Analytical Anisotropic Algorithm (AAA) is a dose calculation model with a 3D pencil beam used in

Varian's Eclipse treatment planning system. It is a convolution-superposition algorithm with a configuration algorithm and the actual dosage evaluation [8].

This method takes into consideration the effects of the presence of heterogeneities by convolutional energy distribution owing to primary particles with a "kernel" describing the dose distribution by secondary particles [9]. This method takes into consideration the effects of the presence of heterogeneities by convolutional the energy distribution owing to primary particles with a "kernel" describing the dose distribution by secondary particles. It accounts for the approximate lateral transit of electrons in the presence of heterogeneity. This is the case AAA of Eclipse TPS (Varian) [9-13] equation 1. A superposition of the various dosage contributions from the primary photons yields the final dose $D(\vec{X}, \vec{Y}, \vec{Z})$ at any arbitrary calculation location in the patient (ph1), contaminated electrons, and extra-focal

*Corresponding Author: Tel: +201002247376; Email: ah_ali2050@yahoo.com

photons (ph2) from all individual beamlets marked by index β [14].

$$D(\vec{x}, \vec{y}, \vec{z}) = \sum_{\beta} (D_{ph1,\beta}(\vec{x}, \vec{y}, \vec{z}) + D_{ph2,\beta}(\vec{x}, \vec{y}, \vec{z}) + D_{cont,\beta}(\vec{x}, \vec{y}, \vec{z})) \quad (1)$$

The computed dose can be described as exposure to water, rescaled according to the specific density, because AAA does not account for chemical material tissue properties [12,15,16].

AXB Dose Calculation Algorithm

Acuros XB algorithm is a deterministic algorithm that can be solved using Boltzmann equation approximations taking into account the lateral electron transport as well as dosage computation affected by heterogeneity [[9,10,17-19]. The algorithm uses the Fokker-Planck equation (describing the spatially and temporally evolution of the probability density of a type of particle) to solve the particle transport. The problem can be solved fast on a computer and is extremely close to a Monte Carlo calculation [20,21]. Two models can describe AXB implementation: photon beam source and radiation transport models. Vassiliev et al [20] initially reported the latter, which comprises discretization of the spatial (\vec{r}), energy (E), and angular (Ω) variables and it was reported in a previous article on Acuros XB validation in water for simple fields [15,16,22].

$$D_i = \int_0^{\infty} dE \int_{4\pi} d\Omega \frac{\sigma_{ED}^e(\vec{r}, E)}{\rho(\vec{r})} \psi^e(\vec{r}, E, \Omega) \quad (2)$$

Where σ_{ED}^e the macroscopic electron cross-section, ψ^e the angular electron fluence and \vec{r} is the material density. Based on the material properties of the patient as derived from the Hounsfield Unit (HU) of

the computed tomography (CT) dataset, Acuros XB calculates the energy-dependent electron fluence [21].

Materials and Methods

The planning system used in this study is Eclipse TPS (treatment planning system) Version V15.6 (Varian Medical Systems, Palo Alto, CA). All stages generated in this work are done using TrueBeam STx HD120 MLC Varian linear accelerator 6MV simulated beams.

The current dosimetry study included computed tomography of 27 patients who had non-small cell lung cancer (NSCLC). Plans were introduced using AAA and AXB. Intensity modulated radiotherapy (IMRT) plans and 3D-prescribed 45Gy dose in 3 fractions, specified in 95% isodose covering 95% Planning target volume (PTV) for 130% of the dose centrally in the tumor.

The computational grid size was 0.25mm for SBRT plans. All of these patients are already being treated with IMRT using a prescribed AAA dose calculation algorithm. NSCLC patients with early-stage (stage I / II) of various locations and locations in the lung that was medically inoperable or the patient voluntarily dropped out of surgery.

SBRT plans introduced retrospectively using AAA and Acuros XB (AXB)[19], were done to assess the difference in the calculations. Parameters used for comparison are Conformity index (CI), Homogeneity Index (HI), Gradient Index (GI), Target mean dose, and calculation time. Dose distribution at isocenter planes was exported to the portal dosimetry application to do the gamma index comparison [20]. The gamma parameters are 2mm and maximum gamma 2%; figure 1 shows the portal dose measurements.

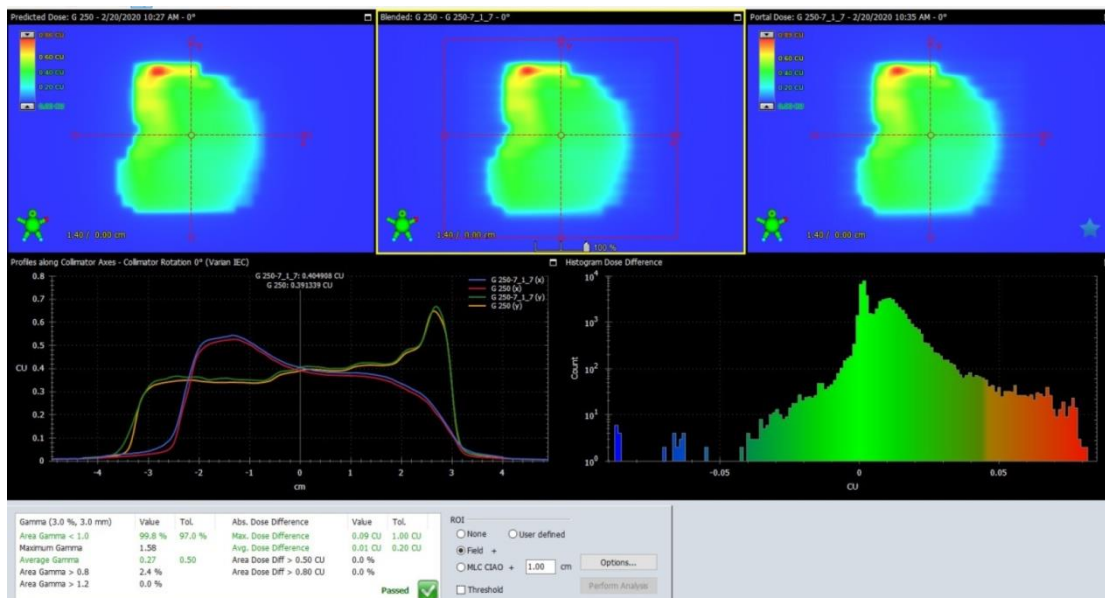


Figure 1. Screenshots for portal dosimetry analysis for planned dose versus measured dose (matching profiles). (A) on the left show the predicted dose from calculated plan (B) in the middle explain the registration between predicted and measured dose (c)on the right is measured dose (D) on the bottom combined profile of the predicted and measured dose and Histogram difference

Treatment plans were studied using the dose distribution, mean dose, conformity index (Equation 3), homogeneity index (Equation 4) for PTV, and Gradient index (GI) (Equation 5) [9].

Due to the existence of low-density lung tissue surrounding the target volume, the accuracy of dose distribution may well be especially difficult in the case of thoracic malignancies for tiny targets, see figure 2.

Conformity index: is the ratio between the reference volume V95% and the volume of PTV [9].

$$CI = \left(\frac{V_{95\%}}{V_{PTV}} \right) \tag{3}$$

There is another definitions to estimate the conformity index by Lomax and Scheib, proposed the Radiation therapy oncology group (RTOG) conformity index [22-24]. Their index is a variation of the Saint-stereotactic Anne's plan quality criterion, for arteriovenous malformations, the Lariboisiere, Tenon (SALT) group was formed [25]. The modified index of Lomax and Scheib, CI Lomax conformity index is calculated as follows:

$$CI = \left(\frac{TV_{PIV}}{PIV} \right) \tag{4}$$

Where TV_{PIV} is the target volume defined by a certain isodose, PIV is the target volume that receives a certain dose and See figure 3.

Homogeneity index: it is, As defined by the International Commission on Radiation Units and Measurements (ICRU) report 83, the difference between the near-maximum dose (D2%) and the near-minimum dose (D98%) divided by the median dose (D50%) [9,26], see figure 4.

$$HI = \left(\frac{D_{2\%} - D_{98\%}}{D_{50\%}} \right) \tag{5}$$

Dose-gradient (GI) can be determined by the volume enclosed by the isodose hypersurface at half the specified dose (PIV half) and the volume encompassed by the isodose hypersurface with the prescribed dose (PIV) [20,26], see figure 5.

The conventional GI is defined as follows:

$$GI = \frac{PIV_{50\%}}{PIV_{100\%}} \tag{6}$$

Where PIV50% is the prescription isodose volume at half prescription isodose and PIV100%, is the total prescription isodose volume [2].

To assess the dose calculation accuracy, a comparison between dose calculation and dose measurement was done. Dose calculations were done for different setups and dose measurements were done using an ion chamber at the calculated points. Dose evaluations were done using a virtual phantom that was created in the TPS. The phantom dimension is 30 × 30 × 30 cm3 and the calculation points were placed on the central axis, directly under different air gaps depth, at 10 cm depth. The air gaps (i.e. low electron density material 0.26 to 0.45g/cm3) were 1.5, 2.5, 3, 4.5, 5, 6.5, 7cm thicknesses. The dose calculations were done for these depths for 100 MU 10x10 cm2 field size at a 100 cm Source skin distance (SSD) setup. Then, the calculated dose using two dose calculation algorithms as compared to the measured dose by cylindrical chamber 0.6cc model (31013 farmer type chamber -PTW).

Statistical analysis

Statistical analysis was performed with Microsoft 2010 Excel sheet applying two-sample t-test and the differences of various parameters of the two groups (where P<0.05) was considered statistically significant.

Results

Dose distribution

Dose distribution is available for visual inspection. Most of the time, routine clinical planning results figure 2 show dose distribution for two different PTV covered with 95%.

Figure 3 shows the variation between the calculated CI of the two calculation algorithms for the 27 patients.

Figure 4 shows the HI calculated for the two-dose calculation algorithms for all 27 patients. In figure 5 see the dose gradient for the two algorithms.

Figure 2. Two different PTV sites for lung cancer and dose distribution coverage of 95% from the prescribed dose for each one.

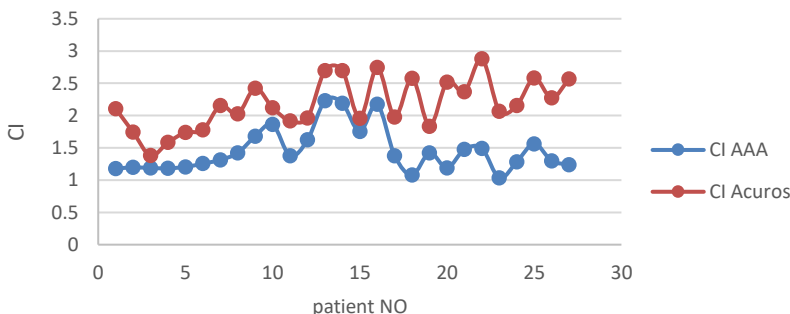


Figure 3. The comparison between conformity indexes for AAA algorithm versus AXB algorithm

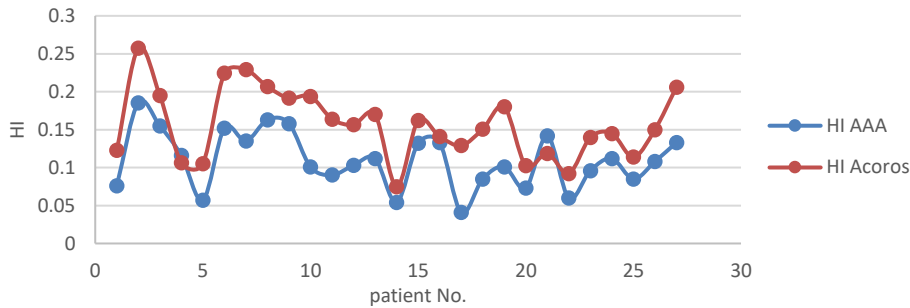


Figure 4. Comparison between homogeneity index for AAA versus AXB algorithm for PTV coverage evaluation.

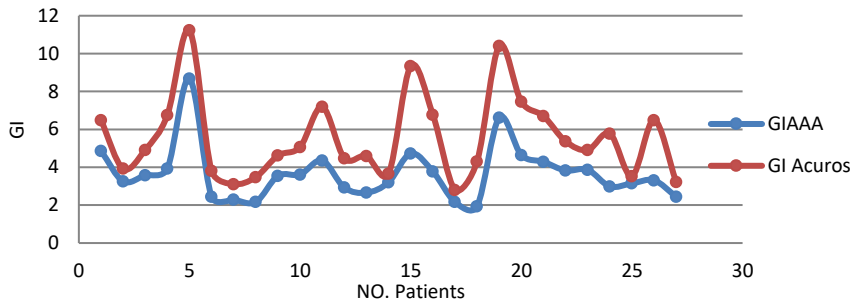


Figure 5. Difference between gradient index for both Algorithms for PTV coverage evaluation

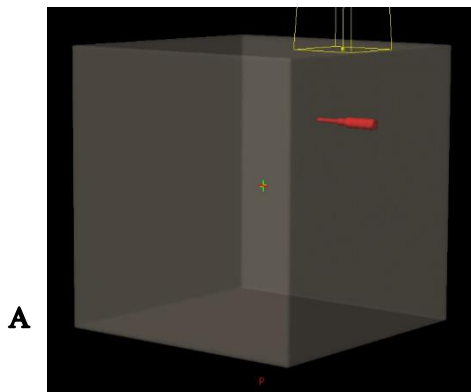


Figure 6. measurement dose for different air gaps and the same depth for ion chamber. A on the left shows the different gaps inserted in the phantom. B on the right shows the position of ion-chamber in the phantom

The Figure 6 shows the TPS calculation setups at different measurement points.

Table 1 Summaries the differences among the measured and calculated doses beneath distinct low-density cloth depths that had been illustrated in Figure 6.

Table 1 Indicates the distinction in measurements and calculation between the two algorithms.

Depth (air cavity) (cm)	1.5	2.5	3	4	5	6.5	7
AAA(%)	-0.7	1.6	2.2	3.4	3.6	3.6	3.3
AXB(%)	0.6	0.9	0.3	0.5	0.4	0.8	0.8

Table 2. Comparisons between AAA and AXB algorithms for evaluation coverage PTV

	AAA	AXB	P-value
CI	1.45±0.55	1.85±0.7	< 0.05
HI	0.15±0.07	0.13±0.08	< 0.05
GI	4.8±2.6	7.4±3.8	< 0.05
Mean dose (%)	95.1±3.3	92.6±3.7	< 0.05
Max dose (%)	2.2±1.6	1.8±0.6	< 0.05
Calculation time (sec)	153±43	185±76	< 0.05

Discussion

The increased CI from AAA to Acuros XB dose calculation algorithms indicate that the calculated dose using AAA is overestimating the dose calculation which means the PTV volume that is assumed to receive 95% dose based on AAA calculations is receiving less in reality. Also, Table 2 can be observed in the HI calculation. That means the homogenous dose that is observed in AAA calculation is not as homogenous as TPS shows. The local gamma criteria confidence limit for portal dosimetry was found to be 3.0% (i.e., 97.0% passing). The findings show the significance of gamma analysis using the method for the accurate estimation of the calculations dose. In 94% of situations, a passing rate of 95% is attained, which is an appropriate level of accuracy for the studied plans, ensuring the IMRT treatment technique employs portal dosimetry.

Results are given in Table 1 show that the phantom dose evaluated by the AXB dose calculation algorithm is closer to the measured dose than the dose evaluated by AAA for the location underneath the low-density volume.

The AXB algorithm accounts for each voxel to offer precise dose calculation in a heterogeneous medium. One of the new features of Eclipse is the improved voxel density to the biological material assignment. The AXB (Advanced type b) algorithm solves the coupled system of linear Boltzmann transport equations (LBTEs), which represents the macroscopic behavior of radiation particles as they move through and interact with matter, in a deterministic manner. In lung SBRT patients with compromised pulmonary function, the AXB algorithm should be used to its advantage. As the model is required to address lateral scaling of electron transport due to locally fluctuating heterogeneities, current AAA and other algorithms of its generation (type A) have intrinsic limitations in heterogeneous media. As the model is required to address lateral scaling of electron transport due to locally fluctuating heterogeneities, current AAA and other algorithms of its generation (type A) have intrinsic limitations in heterogeneous media [21-29]. The AAA and AXB plans were analyzed for the clinical trial based on the data produced from the Dose Volume Histogram (DVH) in the Eclipse TPS by the identical plan except for the calculation algorithm. The mean dose and conformity index at the target volume were significantly different for all 27 patients in this study, as shown in table (2) ($p < 0.05$) for both of the algorithms (AAA and AXB). This outcome is consistent with the findings of various studies. The findings are in agreement with those of other investigations [910,16,25]. However, The Homogeneity Index (HI) showed a statistically significant difference between the two algorithms ($P < 0.05$), AAA had a greater HI than AXB. Several studies have described a similar outcome. [2,13,19,20,25-32].

Conclusion

The consequences of our measurements phantom study confirmed an excellent agreement with calculations performed with the AXB set of rules. A little worse settlement became obtained for the AAA algorithm. The consequences of our scientific examination showed no large variations for the suggested dose and conformity index on the target extent for both algorithms; but, the Homogeneity Index and Maximum Dose are significantly distinct.

AXB is precise for calculating small field doses, especially when employing the SBRT approach. This paper recommends that for SBRT treatment planning dose calculations for low-density tissues as in lung cases and various tumor sites involve tissue heterogeneities, which involves low-density (air) medium and small fields causing charge particle disequilibrium near the air/tissue interface for situations involving small fields like IMRT and low-density density tissue.

Acknowledgment

The authors thank my colleges at Fayoum oncology center for help and support and M. van Wieren for their assistance during the measurements.

References

1. Timmerman RD, Park C, Kavanagh BD. The North American experience with stereotactic body radiation therapy in non-small cell lung cancer. *Journal of Thoracic Oncology*, 2007; 2(7): S101-12.
2. Pizzutiello R, Svatos M. SU-A-BRE-01: AAPM Medical Physics Student Meeting. *Medical Physics*. 2014; 41(6Part2):89.
3. SRS SR. Stereotactic Radiosurgery (SRS) and Stereotactic Body Radiation Therapy (SBRT).
4. Onishi H, Shirato H, Nagata Y, Hiraoka M, Fujino M, Gomi K, et al. Hypofractionated stereotactic radiotherapy (HypoFXSRT) for stage I non-small cell lung cancer: updated results of 257 patients in a Japanese multi-institutional study. *Journal of thoracic oncology*. 2007; 2)7(: S94-100.
5. Partridge M, Ramos M, Sardaro A, Brada M. Dose escalation for non-small cell lung cancer: analysis and modelling of published literature. *Radiotherapy and Oncology*. 2011; 99)1(: 6-11.
6. Wulf J, Baier K, Mueller G, Flentje MP. Dose-response in stereotactic irradiation of lung tumors. *Radiotherapy and oncology*. 2005; 77(1): 83-7.
7. Bezjak A, Paulus R, Gaspar LE, Timmerman RD, Straube WL, Ryan WF, et al. Primary study endpoint analysis for NRG Oncology/RTOG 0813 trial of stereotactic body radiation therapy (SBRT) for centrally located non-small cell lung cancer (NSCLC). *International Journal of Radiation Oncology• Biology• Physics*. 2016; 94(1): 5-6.
8. Sievinen J, Ulmer W, Kaissl W. AAA Photon Dose Calculation Model in Eclipse. 2005;118:2894.
9. Krabch ME, Chetaine A, Nourreddine A, Er-Radi FZ, Baddouh L. Comparative study between Acuros XB algorithm and Anisotropic Analytical Algorithm in the case of heterogeneity for the treatment of lung cancer. *Polish Journal of Medical Physics and Engineering*. 2018; 24(3):115-9.
10. Alghamdi S, Tajaldeen A. Evaluation of dose calculation algorithms using different density materials for in-field and out-of-field conditions. *Exp oncol*. 2019; 41(1): 46-52.
11. Menzel Hans-Georg. International commission on radiation units and measurements. *Journal of the ICRU*. 2014;14(2):1-2.
12. Fogliata A, Nicolini G, Clivio A, Vanetti E, Cozzi L. Dosimetric evaluation of Acuros XB Advanced Dose Calculation algorithm in heterogeneous media. *Radiation oncology*, 2011; 6)1(: 1-15.
13. Kan MW, Leung LH, So RW, Yu PK. Experimental verification of the Acuros XB and AAA dose calculation adjacent to heterogeneous media for IMRT and RapidArc of nasopharyngeal carcinoma. *Medical physics*, 2013; 40(3): 031714.
14. Tillikainen L, Siljamäki S, Helminen H, Alakuijala J, Pyyry J. Determination of parameters for a multiple-source model of megavoltage photon beams using optimization methods. *Physics in Medicine & Biology*, 2007; 52(5): 1441.
15. Tillikainen L, Helminen H, Torsti T, Siljamäki S, Alakuijala J, Pyyry J, et al. A 3D pencil-beam-based superposition algorithm for photon dose calculation in heterogeneous media. *Physics in Medicine & Biology*, 2008; 53(14): 3821.

16. Alagar AG, Mani GK, Karunakaran K. Percentage depth dose calculation accuracy of model based algorithms in high energy photon small fields through heterogeneous media and comparison with plastic scintillator dosimetry. *Journal of applied clinical medical physics*, 2016;17(1):132-42.
17. Mishra P, Li R, Mak RH, Rottmann J, Bryant JH, Williams CL, et al. An initial study on the estimation of time-varying volumetric treatment images and 3D tumor localization from single MV cine EPID images. *Medical physics*, 2014; 41(8Part1): 081713.
18. Tajaldeen A, Ramachandran P, Alghamdi S, Geso M. On the use of AAA and AcurosXB algorithms for three different stereotactic ablative body radiotherapy (SABR) techniques: Volumetric modulated arc therapy (VMAT), intensity modulated radiation therapy (IMRT) and 3D conformal radiotherapy (3D-CRT). *Reports of Practical Oncology and Radiotherapy*. 2019; 24(4):399-408.
19. Tsuruta Y, Nakata M, Nakamura M, Matsuo Y, Higashimura K, Monzen H, et al. Dosimetric comparison of Acuros XB, AAA, and XVMC in stereotactic body radiotherapy for lung cancer. *Medical physics*, 2014; 41(8Part1): 081715.
20. Vassiliev ON, Wareing TA, McGhee J, Failla G, Salehpour MR, Mourtada F. Validation of a new grid-based Boltzmann equation solver for dose calculation in radiotherapy with photon beams. *Physics in Medicine & Biology*. 2010; 55(3): 581.
21. Fogliata A, Lobefalo F, Reggiori G, Stravato A, Tomatis S, Scorsetti M, et al. Evaluation of the dose calculation accuracy for small fields defined by jaw or MLC for AAA and Acuros XB algorithms. *Medical physics*. 2016; 43(10): 5685-94.
22. Krishna GS, Srinivas V, Reddy PY. Clinical implications of Eclipse analytical anisotropic algorithm and Acuros XB algorithm for the treatment of lung cancer. *Journal of medical physics*. 2016;41(4):219.
23. Aristophanous M, Rottmann J, Court LE, Berbeco RI. EPID-guided 3D dose verification of lung SBRT. *Medical physics*. 2011;38(1): 495-503.
24. Wilke L, Andratschke N, Blanck O, Brunner TB, Combs SE, Grosu AL, et al. ICRU report 91 on prescribing, recording, and reporting of stereotactic treatments with small photon beams. *Strahlentherapie und Onkologie*. 2019; 195(3): 193-8.
25. Lomax NJ, Scheib SG. Quantifying the degree of conformity in radiosurgery treatment planning. *International Journal of Radiation Oncology* Biology* Physics*, 2003; 55(5):1409-19.
26. ICRU report 83: Prescribing, Recording and Reporting Photon-Beam Intensity Modulated Radiation Therapy (IMRT). *Journal of the ICRU*. 2010;10(1):1-3
27. Vassiliev ON, Kry SF, Wang HC, Peterson CB, Chang JY, Mohan R. Radiotherapy of lung cancers: FFF beams improve dose coverage at tumor periphery compromised by electronic disequilibrium. *Physics in Medicine & Biology*. 2018; 63(19): 195007.
28. Paddick I, Lippitz B. A simple dose gradient measurement tool to complement the conformity index. *Journal of neurosurgery*. 2006; 105(Supplement):194-201
29. Kan MW, Leung LH, Yu PK. Dosimetric impact of using the Acuros XB algorithm for intensity modulated radiation therapy and RapidArc planning in nasopharyngeal carcinomas. *Int J Radiat Oncol Biol Phys*. 2013;85(1):e73-80.
30. Do Park, Kim TG, Kim JE. Dosimetric impact of intermediate dose calculation for optimization convergence error. *Oncotarget*. 2016; 7(25):37589.
31. Rana S, Rogers K, Pokharel S, Lee T, Reed D, Biggs C. Acuros XB algorithm vs. anisotropic analytical algorithm: a dosimetric study using heterogeneous phantom and computed tomography (CT) data sets of esophageal cancer patients. *Journal of Cancer Therapy*. 2013; 4(1):138-44.
32. Liu HW, Nugent Z, Clayton R, Dunscombe P, Lau H, Khan R. Clinical impact of using the deterministic patient dose calculation algorithm Acuros XB for lung stereotactic body radiation therapy. *Acta Oncologica*. 2014; 53(3):324-9.